Are we ready for offsets up to 50 km? Exploring very far and extremely far offsets in subsalt imaging

Min Yang, Chi Chen, Nicolas Chazalnoel (CGG); Rachel Ho, Bernard P. Laugier (ExxonMobil)*

Summary

Various far-offset marine acquisition geometries have been deemed as promising for alleviating imaging difficulties in the deepwater Gulf of Mexico (GOM). In this case study from the GOM we explore the benefits of far offsets using ocean bottom node (OBN) data with acquisition offsets up to 25 km, and investigate the untapped potential of extremely far offsets of up to 50 km. Using offsets between 12 km and 25 km is not straightforward but these offsets can significantly improve the subsalt images and were valuable for building the salt model in this study. Although their usefulness may be limited in salt model building, we observed imaging benefits from extremely far offsets up to 50 km.

Introduction

Seismic imaging in the deepwater Gulf of Mexico (GOM) has advanced greatly in recent years due to significant progress in seismic acquisition and processing technologies. Nevertheless, subsalt imaging remains challenging beneath complex salt structures, largely due to subsurface illumination limitations and multiple contamination. Acquisition studies based on synthetic modelling have shown that longer offsets and richer azimuths can help subsalt imaging and have led to new acquisition designs, especially for streamer surveys (Moldoveanu and Kapoor, 2009; Mandroux et al., 2013; Long et al., 2014). Deepwater OBN surveys, an acquisition option well suited for subsalt imaging in the GOM, are gaining popularity because of their benefits in flexible acquisition geometry for obstructed oil fields, good repeatability for 4D studies, and full-azimuth coverage with far offsets and high fold. Some studies have already been performed to demonstrate the improvements in model building and seismic imaging with OBN data in complex salt areas (Roberts et al., 2011; Beal et al., 2014; Kristiansen et al., 2014). However, their focus was not around imaging with far-offset data. Most of the studies mentioning the benefits of far offset acquisitions are for velocity model building through full waveform inversion (FWI) (Mothi et al., 2013; Vigh et al., 2013) and for imaging using synthetic data (Li et al., 2009; Li et al., 2010). Only a few found benefits when imaging field data (Wang et al., 2014), likely due to the very low signal-to-noise ratio (S/N) of the far offsets in field data. Synthetic data are usually free of noise and the severe effects of absorption and dispersion, which plague the far offsets in field data. In this study, we focused on exploring and optimizing the benefits from far offsets using real OBN data from the deepwater GOM. This study also provided a unique opportunity to test the imaging benefits of extremely far offsets up to 50 km.

Imaging benefits from very far offsets

An OBN survey was acquired in the deepwater GOM to improve the subsalt image in a geologically complex region. This survey provided full azimuth coverage up to 12 km. Because of its particular acquisition configuration, it also provided limited azimuth data along the shot line direction with offsets up to 25 km, as seen in the rose diagram of Figure 1. Downgoing wavefield data after demultiple were used for our study (Figure 1).

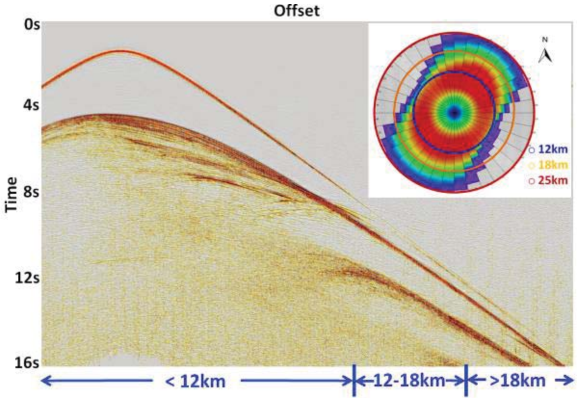

Figure 1: An example node gather of the downgoing wavefield after the demultiple process and OBN rose diagram.

We refer to the survey’s full-azimuth coverage as the regular offset range (0-12 km). As seen on Figure 1, in the range beyond the regular offsets, visible events are residual multiples, together with the direct arrival and water-bottom reflector. Since the far offset (> 12 km) data travel longer in the subsurface than the near offset data, their reflected events are weaker in amplitude than the same events recorded by the regular offsets. Moreover, only offsets up to 12 km have full azimuth coverage. Therefore, simply migrating all offset ranges together does not generally produce many benefits from offsets greater than 12 km.

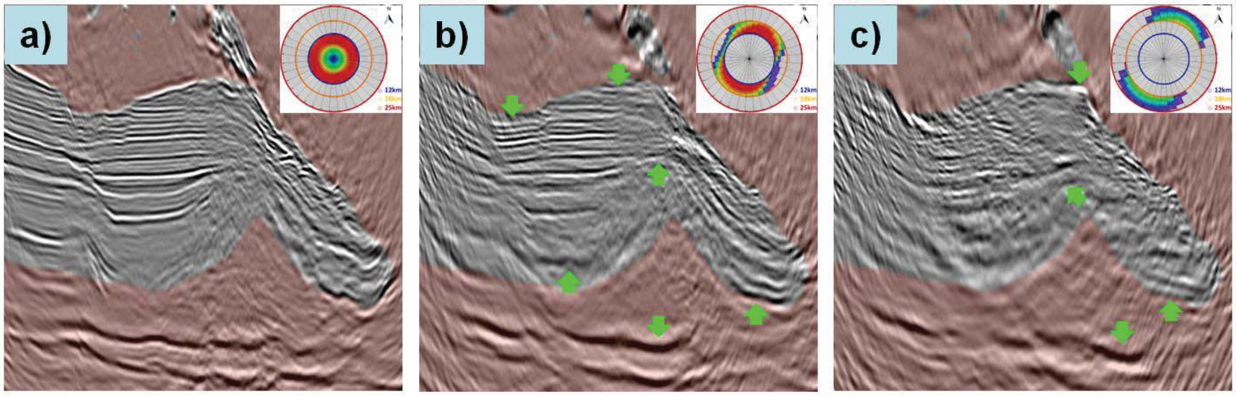

Figure 2: RTM stack with data from (a) regular offsets (0~12 km); RTM from offset ranges of (b) 12-18 km and (c) 18-25 km. A 5000 m gate AGC was applied to normalize group amplitude levels. Green arrows indicate supplemental information provided by far offsets.

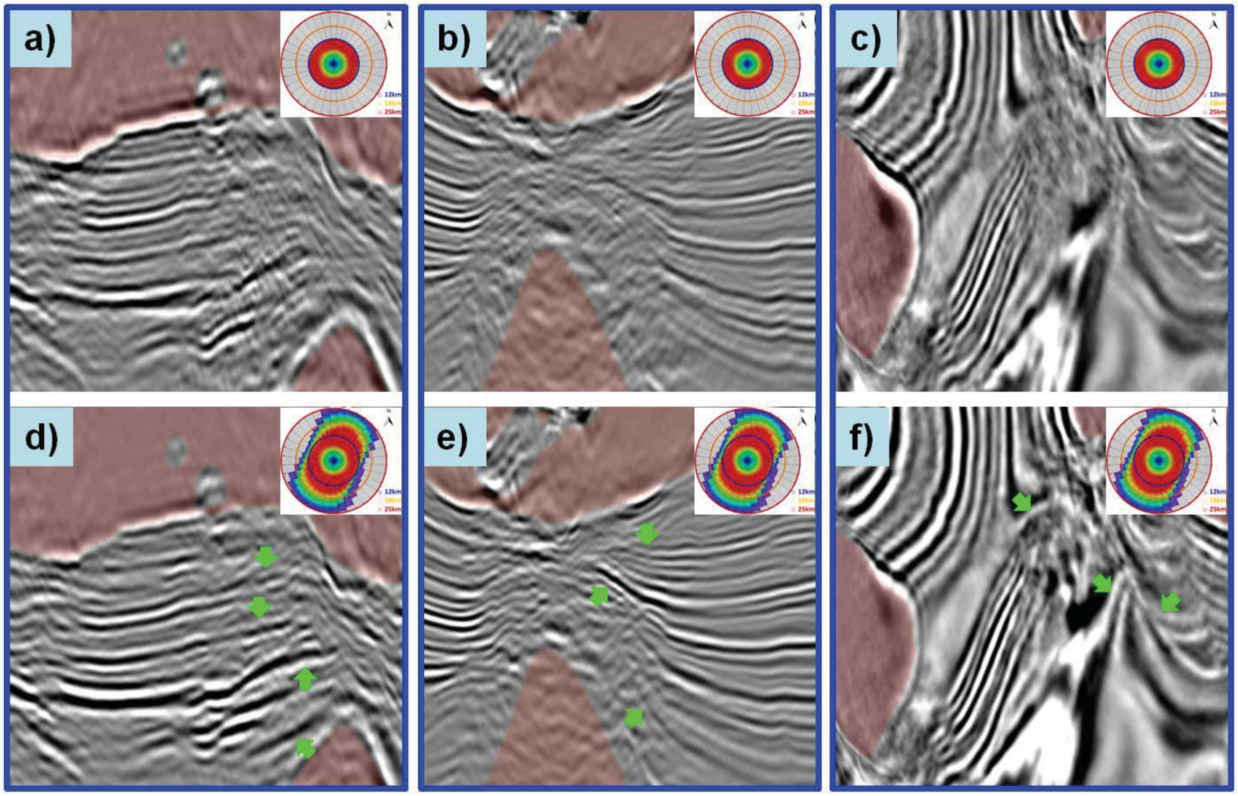

Figure 3: RTM stack (a) inline, (b) crossline, (c) depth slice with regular offsets; RTM stack (d) inline, (e) crossline, (f) depth slice with all offsets using post-migration iterative summation method. A 5000 m gate AGC was applied to normalize the amplitude levels for display. Green arrows indicate improvements due to the very far-offset contribution.

To explore the potential benefits of far offsets, we examined the data in different offset groups. As mentioned earlier, the primaries at the very far offsets were weak and had a poor S/N, and thus required further pre-migration denoise to attenuate residual multiple and mode-converted energy. Here we performed denoise in the tau-p domain to attenuate the residual noise and applied an amplitude balancing to boost the weak signal of the very far offsets. Figure 2 shows RTM images from three different offset ranges (up to 12 km, 12 km to 18 km, 18 km to 25 km). We applied post-migration automatic gain control (AGC) with a 5000 m window to normalize the display of each offset range. Although the full azimuth coverage up to 12 km offsets provided the bulk of the subsalt image, far offsets offered different illumination angles and thus provided supplemental information of the subsalt structures, as highlighted in Figures 2b and 2c (green arrows). The contribution to the subsalt image from the 18-25 km offsets was smaller than that from 12-18 km.

Despite the apparent recovered signal in the RTM result using far offsets, the images had lower frequency content and exhibited timing or phase differences from the regular-offset RTM. Imperfection of the velocity/anisotropy model and improper compensation for the wavelet distortion caused by the earth's dissipative effects were likely among the reasons for this observation. These differences made it challenging to incorporate the far offsets during imaging. An iterative post-migration method of matching and dynamic warping to the regular-offset image was used to maximize the benefits from very far-offset OBN data. Figure 3 shows an inline, a crossline, and a depth slice of the RTM stack with regular offsets and the RTM stack with all offsets that used the post-migration summation method to incorporate the far offsets. Significant improvements in subsalt imaging were observed (green arrows in Figure 3).

Going to extremely far offsets

During the acquisition of this OBN survey, another acquisition was shooting over 30 km away with considerable overlapping time, resulting in significant seismic interference in the recorded node data. Normally, this type of seismic interference would be treated as noise and attenuated at an early stage of the processing. However, this scenario could also be considered as a simultaneous-source acquisition, offering a unique opportunity for experimenting with extremely far-offset data. Iterative deblending was applied to separate the energy from the two sources, thus providing extremely far-offset data up to 50 km to use for testing. Figure 4a shows an example node gather with normal signal and heavy seismic interference from another source. Noise-free signal from one source (Figure 4b) and extremely far-offset "test" data from the other source (Figure 4c) were obtained. As seen from Figure 4c, in the extremely far offsets the strongest events are, again, the direct arrival, the water bottom, and all orders of water-bottom multiples. Determining if any useful information is actually present in the data was difficult. Figure 4d shows the rose diagram of the extremely far-offset test data; the data are mostly in the offset range of 25-50 km and have azimuth coverage predominantly in one direction.

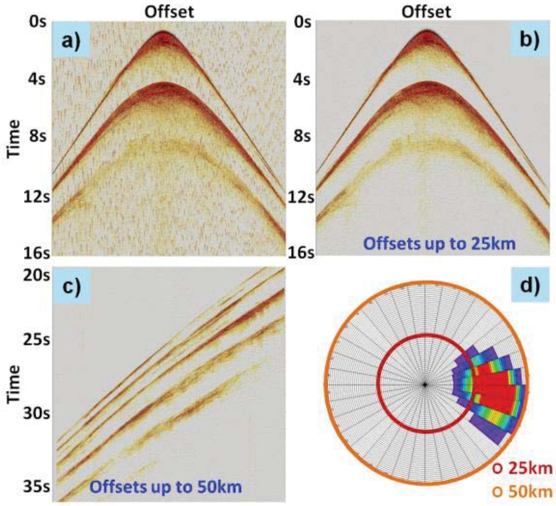

Figure 4: Node gathers illustrating (a) blended data with recording of two unintentionally simultaneous sources; (b) signal from the primary source without seismic interference; (c) extremely far-offset energy from the other source; (d) rose diagram of the extremely far-offset data.

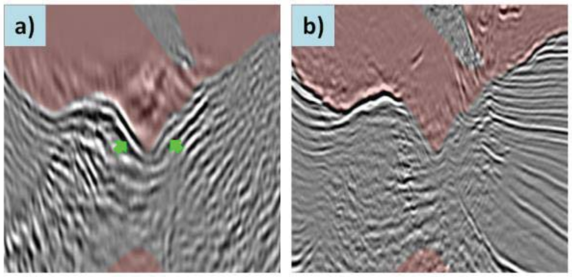

Figure 5: (a) RTM stack of extremely far offsets up to 50 km; (b) RTM stack with WAZ data, offsets up to 9 km. AGC was applied to normalize the amplitude levels. Green arrows indicate the salt keel illuminated by extremely far offsets.

Since the area covered by the sources and receivers of this extremely far-offset data was much larger than the current OBN survey, a salt model developed in earlier imaging of this area with conventional wide-azimuth data was used to test the potential of the extremely far offsets. RTM with extremely far offsets revealed a salt keel image (green arrows in Figure 5a) that was only barely observable on the

RTM image with conventional WAZ data up to 9 km (Figure 5b). Please note that a comparison with the previously used OBN data was not possible due to difference in coverage areas. This test demonstrated that extremely far offsets can provide alternative illumination that could be useful in imaging complex salt bodies.

Discussion

Model building with far offsets on field data has mostly been focused on FWI and tomography for sediment model updates (Vigh et al., 2013; Zdraveva et al., 2015; Wang et al., 2014). In this GOM study we demonstrated the benefits for imaging of salt geometry and subsalt events. Next, we discuss the benefit of using far offsets in building the salt geometry.

To study their potential benefits, experiments with salt flood were conducted for very far (12-25 km) and extremely far offsets (25-50 km). Figure 6 shows a salt flood with regular and very far offsets in a complex salt area. Hardly any indication of base of salt (BOS) can be seen in the salt flood image with regular offsets (Figure 6a), while good indication of base of salt is visible in the image from very far offsets (green arrows in Figure 6b). The very far offsets likely undershot the complex narrow mini-basin directly above it and were able to properly image the BOS.

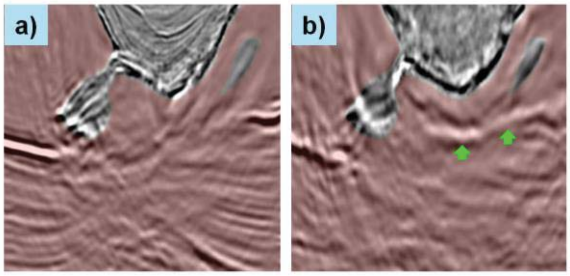

Figure 6: Salt flood RTM with (a) regular offsets of 0-12 km and (b) very far offsets of 12-25 km. The base of salt is much more visible in the image from very far offsets (green arrows).

In the other area where we have extremely far offsets (25-50 km), even though the salt keel was obvious in the salt model migration (Figure 5a), its image mostly disappeared on the salt flood migration (Figure 7a). On the other hand, a salt flood in a much more localized area revealed the BOS again (Figure 7b), indicating that the wave paths imaging the BOS partially travelled through sediments covered by salt in the salt flood scenario. This was consistent with our understanding that the longer the seismic waves travel, the more vulnerable the migration is to the accuracy of the model. In the case of extremely far offsets, even subtle changes of the model along the long path of the wave propagation could poorly position or totally destroy the already-weak events due to ineffective migration focusing. Even with very far offsets, the level of benefits in salt interpretation should drop as the degree of uncertainty in the velocity model increases. To work around this limitation, we built a salt model with full azimuth data up to 12 km offset before exploring the potential of very far offsets in salt model building and subsalt imaging.

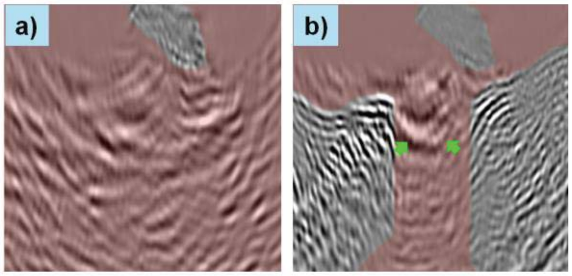

Figure 7: RTM with extremely far offsets (25-50 km): (a) with salt flood model; (b) with keel salt flood model. Extremely long offsets are much more vulnerable to model inaccuracies, explaining why the BOS (green arrows) is visible only in (b).

Conclusions

We used a unique acquisition scenario for an OBN survey in the deepwater GOM to study very far offsets and extremely far offsets. To tackle the very low S/N in very far offsets, we examined the data in different offset groups, performed additional denoise and amplitude balancing for far-offset data, migrated data in three offset ranges, and used a post-migration iterative summation method to maximize the benefits of very far offsets. We demonstrated that, while challenging, very far offsets improved the subsalt image and showed great potential for use in salt model building, in addition to the well-known model building benefits for FWI and tomography. Some benefit was observed from extremely far offsets (up to 50 km) as well, although the benefit was limited due to its magnified dependence on the accuracy of the velocity model.

Acknowledgements

We thank ExxonMobil, FairfieldNodal, and CGG for permission to publish these results. We appreciate the support from the CGG and ExxonMobil teams in this study.

EDITED REFERENCES

Note: This reference list is a copyedited version of the reference list submitted by the author. Reference lists for the 2016 SEG Technical Program Expanded Abstracts have been copyedited so that references provided with the online metadata for each paper will achieve a high degree of linking to cited sources that appear on the Web.

REFERENCES

Beal, E., E. Salo, and C. Corcoran, 2014, Lessons from the deep — processing ocean bottom seismic data: 84th SEG Annual International Meeting, Expanded Abstracts, 3679–3683, http://dx.doi.org/10.1190/segam2014-1420.1.

Kristiansen, P., A. Ogunsakin, M. Esotu, O. Zdraveva, B. Hootman, and E. Quadt, 2014, Deepwater OBN - Exploiting data-processing possibilities: 84th SEG Annual International Meeting, Expanded Abstracts, 4258–4262.

Li, H., J. Kapoor, N. Moldoveanu, and B. Dragoset, 2009, The contribution of longer offsets to subsalt imaging: 79th SEG Annual International Meeting, Expanded Abstracts, 127–131, http://dx.doi.org/10.1190/1.3255085.

Li, H., J. Kapoor, N. Moldoveanu, B. Dragoset, and K. Jiao, 2010, Evaluation of longer offsets to subsalt imaging through elastic modeling: 80th SEG Annual International Meeting, Expanded Abstracts, 3008–3012, http://dx.doi.org/10.1190/1.3513471.

Long, A., S. Campbell, S. Fishburn, S. Brandsberg-Dahl, N. Chemingui, and V. Dirks, 2014, No-compromise marine seismic: A full-azimuth survey design for total-wavefield velocity model building and imaging in the deep-water Gulf of Mexico. 84th SEG Annual International Meeting, Expanded Abstracts, 52–56, http://dx.doi.org/10.1190/segam2014-1022.1.

Mandroux, F., C. Ting, B. Montgomery, and A. Lenart, 2013, Staggered marine acquisition design for complex imaging. 83rd SEG Annual International Meeting, Expanded Abstracts, 26–30, http://dx.doi.org/10.1190/segam2013-0354.1.

Moldoveanu, N., and J. Kapoor, 2009, What is the next step after WAZ for exploration in the Gulf of Mexico? 79th SEG Annual International Meeting, Expanded Abstracts, 41–45, http://dx.doi.org/10.1190/1.3255750.

Mothi, S., K. Schwarz, and H. Zhu, 2013, Impact of full azimuth and far offset acquisition on full waveform inversion in deep water Gulf of Mexico: 83rd SEG Annual International Meeting, Extended Abstracts, 924–928, http://dx.doi.org/10.1190/segam2013-0102.1.

Roberts, M., T. Dy, S. Ji, M. Reasnor, and D. Shepherd, 2011, Improving atlantis TTI model building: OBN NATS, prism waves & 3D RTM Angle Gathers: 81st SEG Annual International Meeting, Expanded Abstracts, 3238–3242m, http://dx.doi.org/10.1190/1.3627868.

Vigh, D., J. Kapoor, and N. Moldoveanu, 2013, Far offset aided full waveform inversion: 13th International Congress of the Brazilian Geophysical Society, 294–297.

Wang, M., Y. (Fred) Li, and Q. Wu, 2014, Impact of ultra-far offsets on tomography and subsalt imaging in deep-water Gulf of Mexico: 84th SEG Annual International Meeting, Expanded Abstracts, 3694–3698.

Wu, Y., K. Jiao, D. Vigh, N. Moldoveanu, X. Cheng, and D. Sun, 2015, Full waveform inversion with glider acquisition: Combination of technology revolutions: 85th SEG Annual International Meeting Expanded Abstracts, 1101–1105, http://dx.doi.org/10.1190/segam2015-5925337.1.

Zdraveva, O., A. Ogunsakin, B. Hootman, P. Kristiansen, and E. Quadt, 2015, Improved imaging of deepwater reservoir by TTI model building and optimized use of OBN data: 85th SEG Annual International Meeting, Expanded Abstracts, 5198–5201.